

1 Article

2 **Physiological and transcriptomic analysis of yellow** 3 **leaf coloration in *Populus deltoides* Marsh**

4 **Shuzhen Zhang**¹, **Xiaolu Wu**¹, **Jie Cui**¹, **Fan Zhang**^{1,*}, **Xueqin Wan**², **Qinglin Liu**¹, **Yu Zhong**²
5 **and Tiantian Lin**²

6 ¹ College of Landscape Architecture, Sichuan Agricultural University, Chengdu 611130, China;
7 limaoxiaojie@126.com (S.Z.); 778020343@qq.com (X.W.); 306946403@qq.com (J.C.); nolady@163.com (F.Z.);
8 279682726@qq.com (Q.L.)

9 ² College of Forestry, Sichuan Agricultural University, Chengdu 611130, China; w-xue@163.com (X.W.);
10 867106174@qq.com (Y. Z.); 120470952@qq.com (T. L.)

11 * Correspondence: nolady@163.com; Tel.: +86-151-9805-0108

12 Received: date; Accepted: date; Published: date

13 **Abstract:** As important deciduous tree, *Populus deltoides* Marsh possesses a high ornamental value
14 for its leaves remaining yellow during the non-dormant period. However, little is known about the
15 regulatory mechanism of leaf coloration in *Populus deltoides* Marsh. Thus, we analyzed
16 physiological and transcriptional differences of yellow leaves (mutant) and green leaves (wild-type)
17 of *Populus deltoides* Marsh. Physiological experiments showed that the contents of chlorophyll (Chl)
18 and carotenoid are lower in mutant, the flavonoid content is not differed significantly between
19 mutant and wild-type. Transcriptomic sequencing was further used to identify 153 differentially
20 expressed genes (DEGs). Functional classifications based on Gene Ontology enrichment and
21 Genomes enrichment analysis indicated that the DEGs were involved in Chl biosynthesis and
22 flavonoid biosynthesis pathway. Among these, geranylgeranyl diphosphate (CHLP) genes
23 associated with Chl biosynthesis showed down-regulation, while chlorophyllase (CLH) genes
24 associated with Chl degradation were up-regulated in yellow leaves. The expression levels of these
25 genes were further confirmed using quantitative real-time PCR (RT-qPCR). Furthermore, the
26 measurement of the main precursors of Chl confirmed that CHLP is vital enzymes for the yellow
27 leaf color phenotype. Consequently, the formation of yellow leaf color is due to disruption of Chl
28 synthesis and catabolism rather than flavonoid content. These results contribute to our
29 understanding of mechanisms and regulation of leaf color variation in poplar at the transcriptional
30 level.

31 **Keywords:** poplar; transcriptome; RNA-Seq; flavonoids; chlorophylls; yellow-green leaf color
32 mutant

33

34 1. Introduction

35 Leaf color is an important feature of ornamental plants, and trees with colored leaves have been
36 widely cultivated in landscape gardens. The main factors that determine foliage color are the types
37 of pigment and their relative concentrations. The formation of red leaves is the result of anthocyanin
38 accumulation, which has been extensively studied [1]. In contrast, there are only a few studies focus
39 on the mechanism of yellow leaves. Leaf yellowing is generally considered to be caused by
40 decreased Chl content, since Chl is the main pigment content of green leaves [2]. Therefore, studies
41 of leaf yellowing have mostly focused on Chl biosynthesis and degradation. In addition, leaf

42 yellowing may be also due to the accumulation of flavonoids such as flavanol, flavonol, chalcone,
43 aurone [3,4].

44 The Chl biosynthetic pathway consists of about 20 different enzymatic steps, starting from
45 glutamyl-tRNA to Chl a and Chl b [5]. Mutations in any one of the genes of the pathway can affect
46 the accumulation of Chl [6], decrease photosynthesis capacity [7] and affect the development of
47 chloroplast [8]. The silence of *CHLD* and *CHLI* (magnesium chelatase subunit D and I) induced by
48 virus in peas resulted in yellow leaf phenotypes with rapid reduction of photosynthetic proteins,
49 undeveloped thylakoid membranes, altered chloroplast nucleoid structure and malformed antenna
50 complexes [9]. Moreover, in rice, *PGL10* encoded protochlorophyllide oxidoreductase B (PORB),
51 pale-green leaf mutant *pgl10* had decreased Chl (a and b), carotenoid contents, as well as grana
52 lamellae of chloroplasts compared with the wild-type [10]. In addition, mutants with disrupted Chl
53 degradation were used to characterize many steps in the Chl degradation pathway in leaves
54 undergoing senescence [11]. In *Arabidopsis* mutant deficient in PPH (pheophytinase), Chl
55 degradation is inhibited, and the plants exhibit a typeC stay-green phenotype during senescence [12].
56 Previous studies revealed that chlorophyllase (Chlase) is involved in Chl degradation in
57 ethylene-treated citrus fruit and could regulate the balance between different plant defense
58 pathways, enhance plant resistance to bacteria [13-15]. Recently, Mutants deficient in Chl
59 biosynthesis and degradation have been identified in many yellow leaf plants, such as rice [16-19],
60 *Arabidopsis thaliana* [20] and pak-choi [21].

61 The genotype we reported is a kind of *Populus deltoides* Marsh (mutant), which is a bud
62 mutation of green leaf *Populus deltoides* Marsh (wild-type) (Figure 1). The mutant is a rare yellow leaf
63 variety which was found in poplar plants of the Salicaceae family. There exists extremely high
64 ornamental value for this species because its leaves remain golden in spring, summer and autumn.
65 However, the molecular mechanism underlying the leaf color of the mutant has not yet been
66 elucidated. Many ornamental plant cultivars with fruit or flower color variation arose from the bud
67 mutation. For instance, the color in grape skin changes from white to red due to bud mutant [22],
68 flower color mutants of roses, carnations and chrysanthemums have also been reported [23]. In
69 contrast, yellow leaf phenotype caused by bud mutant were hardly reported. On the other hand, the
70 study related to yellow leaf color were mostly focused on leaf yellowing. For example, the tea
71 cultivar 'Anji Baicha' produces yellow or white shoots at low temperatures, and turn green when the
72 environmental temperatures increase [24]. Only a few studies have reported the yellow leaf
73 phenotype, such as the cucumber Chl-deficient golden leaf mutation [25].



74

75 **Figure 1.** Phenotype of green leaf and yellow leaf. Bar=5 cm.

76 In this study, the photosynthetic pigments contents, Chl precursors contents, flavonoid contents
77 and transcriptomics of the mutant type and wild type were analyzed. Based on a combination of
78 biochemical analysis and bioinformatics, we identified differentially expressed genes (DEGs related
79 to Chl and flavonoid biosynthesis. Furthermore, the expression of DEGs involved in leaf coloration

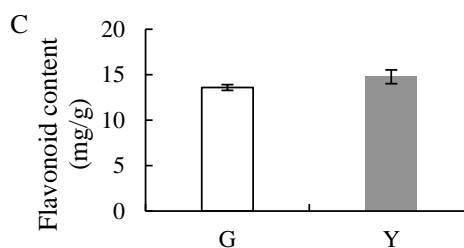
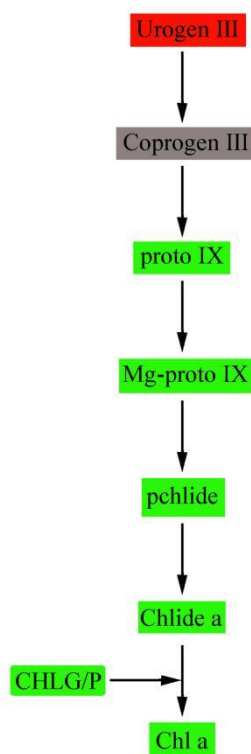
80 was validated using quantitative real-time polymerase chain reaction (RT-qPCR). Our results
81 clarified the physiological and transcriptomic aspects of golden leaf coloration in *Populus deltoides*
82 Marsh and will serve as a platform to advance the understanding of the regulatory mechanisms
83 underlying the leaf color formation in poplar and other plant species.

84 2. Results

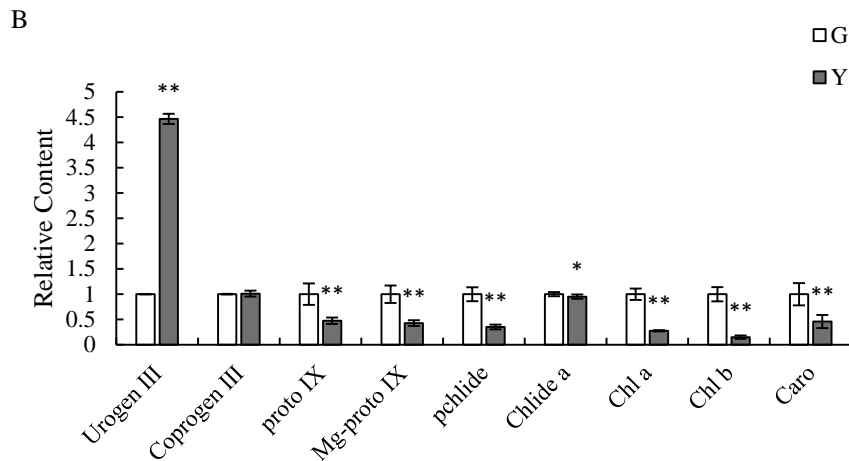
85 2.1. Pigment content analysis of wild-type and mutant

86 We analyzed changes in the pigment contents of wild-type leaves and mutant leaves. The
87 uroporphyrinogen III (Urogen III) content of the yellow leaves was significantly higher than that of
88 the wild-type, whereas there were no significant differences in coproporphyrinogen III (Coprogen
89 III) (Figure 2). Further detailed analysis showed that the protoporphyrin IX (Proto IX), magnesium
90 protoporphyrin IX (Mg-Proto IX) and protochlorophyllide (Pchlde) contents of the mutant were
91 significantly decreased by about 52.53%-64.71% than those from green leaves. On the other hand, the
92 content of chlorophyllide (Chlide) a in yellow leaves was lower than that of green leaves. Compared
93 with the green leaves, the Chl a content, Chl b content and carotenoids content of yellow leaves
94 decreased significantly by 72.41%, 84.86% and 53.88%, respectively (Figure 2). In addition, the
95 difference between the total flavonoid contents of the green leaves and yellow leaves was not
96 significant (Figure 2).

A



97



98

99

100

101

102

103

104

105

106

107

108

Figure 2. Determination of pigment contents in G (green leaves) and Y (yellow leaves). (A) Schematic view of the Chl biosynthesis pathway. The rounded rectangle shows the gene encoding protein catalyzing the reaction of the precursors. The red color means significantly increased in the Y leaves. The green color means significantly decreased or down-regulated in the Y leaves. The gray color means there was no significant difference between the G and Y leaves; (B) Comparison of the relative contents of Chl precursors and photosynthetic pigments; (C) Comparison of the flavonoid contents. Asterisks indicate: (*) $P \leq 0.05$, (**) $P \leq 0.01$. Urogen III, uroporphyrinogen III; Coprogen III, coproporphyrinogen III; Proto IX, protoporphyrin IX; Mg-Proto IX, Mg-protoporphyrin IX; Pchlide, protochlorophyllide; Chlide a, chlorophyllide a; Chl a, chlorophyll a; Chl b, chlorophyll b; Caro, carotenoid.

109

2.2. Analysis of sequencing data

110

111

112

113

114

115

116

117

RNA-seq libraries were constructed from green and yellow leaf samples and sequenced using the Illumina HiSeq™ 4000 platform for acquiring a comprehensive overview of leaf coloration. Approximately 45 million and 47 million raw reads were obtained from each sample. After removal of adaptor sequence and low quality reads, the number of clean reads in the two libraries was 40,779,290 and 41,776,346. The Q20 and Q30 of the two samples were at least 97.28 and 93.20%, respectively, and the GC contents both exceeded 45%. Additionally, 73.79% or 71.67% of reads of each samples were mapped to the *Populus trichocarpa* Torr. & Gray genome sequence and approximately 47% of the mapped reads were uniquely mapped reads (Table 1).

118

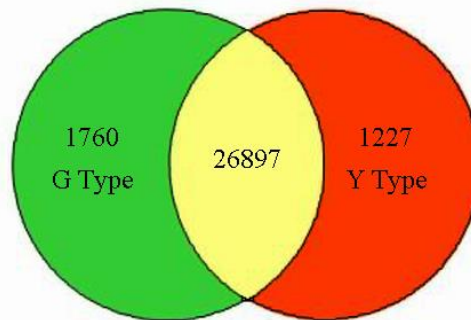
Table 1. Summary of the sequencing and mapping results.

Sample name	G	Y
Raw reads	45846322	47483602
Clean reads	40779290	41776346
Q20(%)	97.45	97.28
Q30(%)	93.57	93.20
GC content(%)	45.36	45.14
Total mapped	30092762(73.79%)	29942722(71.67%)

Uniquely mapped 9961342(48.85%) 9903152(47.41%)

119 2.3. Analysis of gene expression

120 In total, the number of expressed genes were 28,657 and 28,124 in green (G) and yellow (Y)
121 leaves, respectively, of which 1760 and 1227 genes were expressed specifically in the G and Y type
122 (Figure 3). In order to identify DEGs between G and Y, we set the expression of genes in G as the
123 control and identified genes that were up- or downregulated in Y. Accordingly, A total of 153 DEGs
124 were found in Y, including 52 up-regulated genes and 101 down-regulated genes.

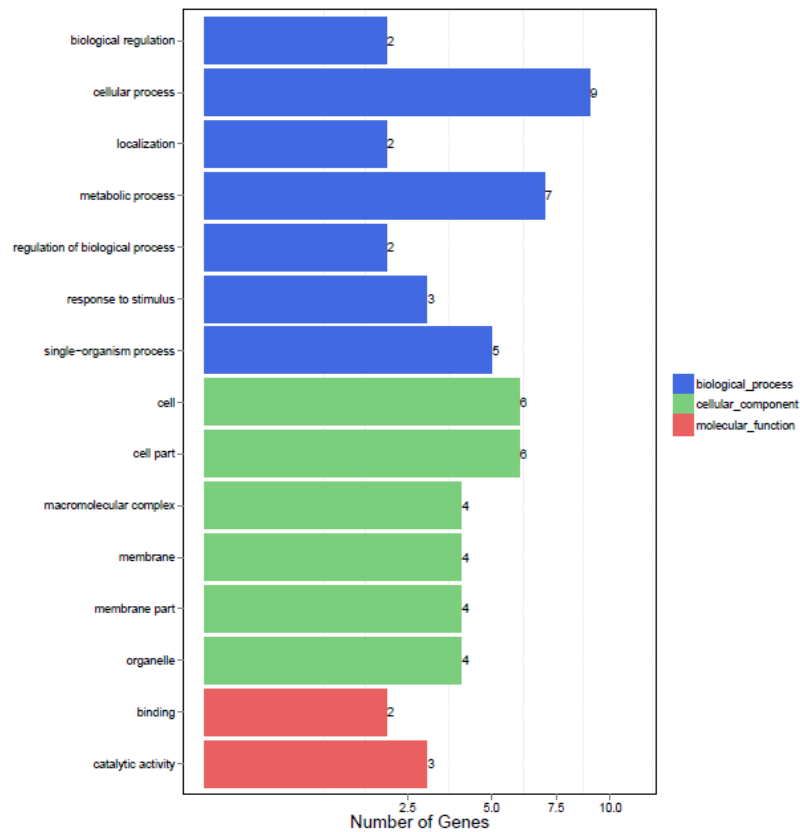


125

126 **Figure 3.** The numbers of specific genes and shared genes between G and Y.

127 2.4. Gene functional annotation by GO, and KEGG

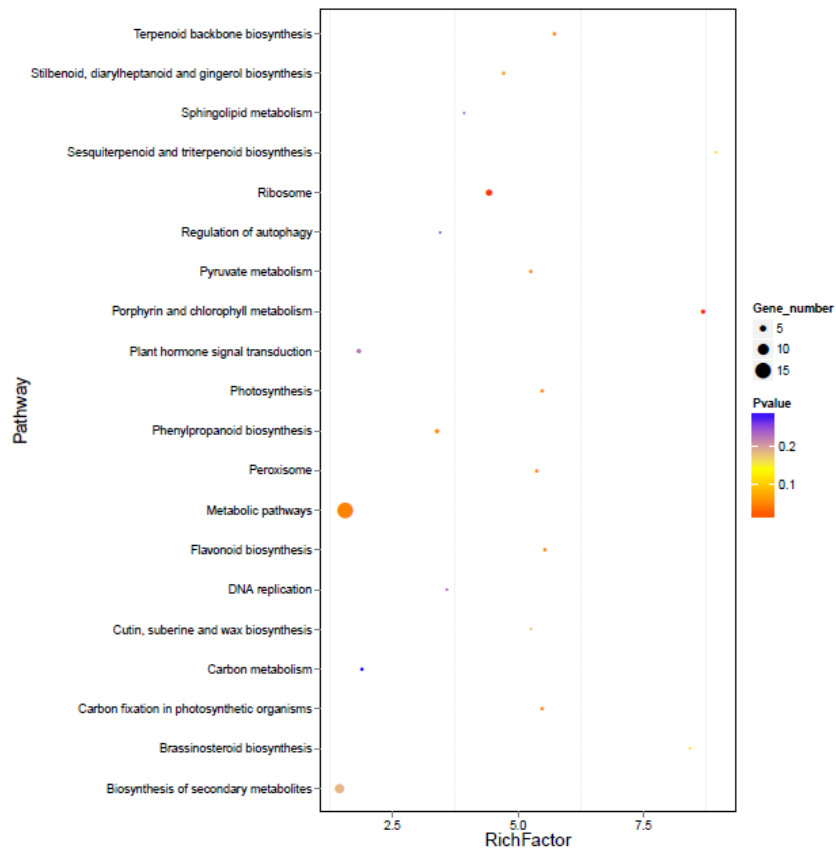
128 GO assignments were used to classify the functions of DEGs. A total of 12, 9, and 5 of the DEGs
129 were divided into biological processes, cellular components and molecular functions respectively,
130 and some DEGs were annotated with more than one GO term (Figure 4). In the biological process
131 category, a large number of DEGs fell into the categories of 'cellular process', 'metabolic process',
132 and 'single-organism process' (Table S1). The most enriched terms of the cellular component were
133 involved in 'cell', 'cell part', and 'membrane', 'membrane part' were also significantly enriched
134 terms (Table S1). Meanwhile, the dominant categories with respect to molecular function group
135 were 'binding' and 'catalytic activity' (Table S1).



136

137 **Figure 4.** The most enriched GO term assignment to DEGs in G and Y. X-axis displays the gene
138 number. The DEGs were annotated in three categories: biological process, cellular component and
139 molecular function (Y-axis).

140 KEGG pathway analysis was performed to categorize gene functions with an emphasis on
141 biochemical pathways that were active in G and Y. A total of 52 genes were annotated and assigned
142 to 31 KEGG pathways (Table S2). The most significantly enriched pathway was 'Metabolic pathways'
143 (Figure 5), with 15 associated DEGs (ranked by padj value), followed by 'Biosynthesis of secondary
144 metabolites' and 'Ribosome' with 8 and 5 DEGs, respectively, which supported the results of GO
145 assignments that 'metabolic process' was significantly enriched. Moreover, 3 DEGs were assigned to
146 'Porphyrin and Chl metabolism' and 2 DEGs were assigned to 'Flavonoid biosynthesis'. This cluster
147 of results indicated that the differences in metabolic activities were the main difference between G
148 and Y, and they may perform important roles in the regulating of leaf coloration.



149

150 **Figure 5.** The enriched KEGG pathways of DEGs. The X-axis displays the Rich factor, and the Y-axis
 151 displays the KEGG pathways. The size of the dot corresponds to the number of DEGs in the pathway,
 152 and the colour of the dot indicates different Q value.

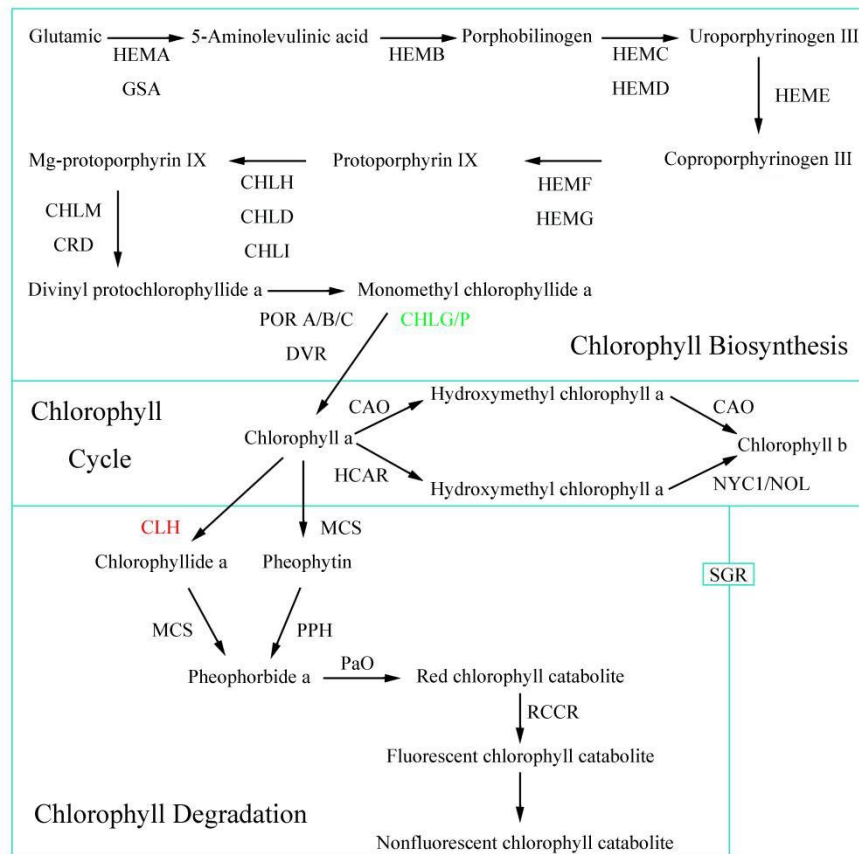
153 *2.5. Analysis on Genes Related to Chl and Flavonoid Biosynthesis*

154 Based on the above annotations, we found that the *Populus deltoides* Marsh transcriptome
 155 database contains genes involving in Chl biosynthesis and flavonoid biosynthesis (Table 2). Two
 156 genes annotated as CHLP (Potri.019G009000 and Potri.019G024600) were down-regulated in Y. In
 157 the last step of Chl a biosynthesis, the geranylgeranyl diphosphate (CHLP, EC:1.3.1.111) catalyzes
 158 the reduction of geranylgeranyl pyrophosphate to phytol pyrophosphate and yields Chl (Figure 6).
 159 Furthermore, the gene encoding Chlase (CLH, EC:3.1.1.14) plays roles in the transition of Chl a(b) to
 160 Chlide a(b), which was found to be up-regulated in Y. In flavonoid biosynthesis, two genes
 161 annotated as HCT were differentially expressed in G and Y. Of these, one gene (Potri.006G034100)
 162 was more highly expressed in G while the other gene (Potri.005G028500) was more highly expressed
 163 in Y.

164 **Table 2.** DEGs involved in Chl and flavonoid biosynthesis in mutant transcriptome.

Function	Gene ID	Seq. Description	log2FC
chlorophyll biosynthesis	Potri.019G009000	GDSL-like Lipase/Acylhydrolase superfamily protein	-10.7764
	Potri.019G024600	GDSL-like Lipase/Acylhydrolase superfamily protein	-10.1319
	Potri.005G214100	chlorophyllase 1	9.6073

flavonoid biosynthesis	Potri.005G028500	HXXXD-type acyl-transferase family protein	9.2808
	Potri.006G034100	HXXXD-type acyl-transferase family protein	-9.8978



165

166

167

Figure 6. DEGs at the transcript level involved in Chl biosynthesis pathways. Up-regulated genes are marked by red and down-regulated genes by green.

168

2.6. Quantitative real-time PCR validation of RNA Sequencing data

169

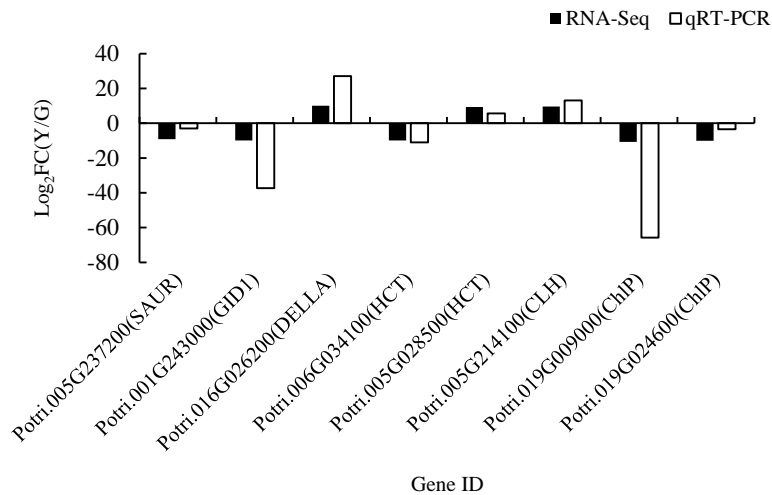
170

171

172

173

To validate the accuracy of RNA-seq expression results, 8 DEGs with marked changes in plant hormone signal transduction, flavonoid biosynthesis and Chl biosynthesis were detected by qPCR (Figure 7). The results showed that except 3 genes (DELLA, HCT, CLH), the remaining 5 genes were all down-regulated in mutant plants. In general, qRT-PCR results concur with the RNA-seq data, indicating that the DEGs identified by RNA-seq were accurate.



174

175 **Figure 7.** RT-qPCR analysis of the expression values of the 8 DEGs in the Y type. Log₂(FC) represents
176 the fold change in Y relative to that in G.

177 3. Discussion

178 The expression of leaf color in the mutants is often influenced by genes involved in the
179 chloroplast development, Chl synthesis and catabolism, or environmental conditions like
180 temperature and light intensity. Of the many rice yellow green leaf mutants, *ygl1* mutant is due to a
181 missense mutation in a highly conserved residue of *YGL1* which encodes the Chl synthase (CHLG)
182 [7], *ygl2* mutant is due to an insert mutation of *YELLOW-GREEN LEAF2* which encodes Heme
183 Oxygenase 1 [26]. The impaired chloroplast development of pak-choi yellow leaf mutant is
184 associated with blocked Chl biosynthesis process [21]. In *Setaria italica*, the chlorotic organs is caused
185 by *EGY1* (ethylene-dependent gravitropism-deficient and yellow-green 1), which results in
186 premature senescence and damaged PS II function [27]. The single incompletely dominant gene
187 *Y1718* that is on chromosome 2BS is responsible for the yellow leaf color phenotype of wheat mutant
188 [28]. As a result of a single nucleotide substitution in the *CsChlI* gene for magnesium chelatase I
189 subunit, the cucumber mutant exhibited the golden yellow leaf color throughout its growth stage
190 [25]. The leaf color in the *Japonica* rice is temperature dependent, the mutant displayed yellow-green
191 leaves at low temperature (20°C) and green leaves at higher temperature (34°C) during the seedling
192 stage [29]. The golden leaves of tropical plant *Ficus microcarpa* L. f. cv. is high-light sensitive, which
193 sun-leaves are yellow and shade-leaves are green [30]. In this study, yellow leaf color of G-type is
194 caused by genes involved in the Chl synthesis and catabolism.

195 3.1. The Expression Level of Genes Involved in Chl Biosynthesis Were Altered in Leaf Color Mutants

196 Leaf color formation is closely related to Chl biosynthesis and breakdown, most leaf color
197 mutations are Chl-deficiency mutations [31]. Chl is responsible for harvesting solar energy and
198 electron transport, even turning plants green because it is Mg²⁺-containing tetrapyrrole pigments
199 [32]. In this study, the novel Chl-deficient chlorina mutant of *Populus deltoides* Marsh with yellow leaf
200 phenotype was identified. Compared with G, the content of photosynthetic pigments in the Y were
201 significantly lower. In particular, the Chl b content were six times higher in Y than G plants. Those
202 results suggesting that the yellow leaf phenotype in mutant is a result of a lack of Chls.

203 The Chl metabolic process can be subdivided into three parts: biosynthesis of Chl a, the Chl
204 cycle between Chl a and b, and degradation of Chl a [33-35]. Chl is composed of two moieties, Chlide
205 and phytol, which are respectively formed from the precursor molecules 5-aminolevulinic acid and
206 isopentenyl diphosphate [36]. *CHLP* encodes the enzyme geranylgeranyl reductase catalysing
207 terminal hydrogenation of geranylgeraniol to phytol for Chl synthesis [37,38]. Previous studies

208 revealed that in transgenic tobacco (*Nicotiana tabacum*) expressing antisense *CHLP* RNA,
209 transformants with gradually reduced *CHLP* expression displayed a uniform low pigmentation and
210 a pale or variegated phenotype [39]. In cyanobacterium *Synechocystis* sp. PCC 6803, $\Delta chlP$ mutant
211 exhibit decreased Chl and total carotenoids contents, and unstable photosystems I and II [40]. Two
212 *CHLP* genes (Potri.019G009000 and Potri.019G024600) were identified in our database, and both
213 were down-regulated in the mutant. In the meantime, qPCR experiment further verified that
214 expression levels of *CHLP* genes in Y were highly reduced compared with those in G, which
215 suggesting that a later stage of Chl biosynthesis was interrupted. Parallel experiments also showed
216 that the content of Chlide a was about 4.83% lower, while the content of Chl a was 72.41% lower in
217 the Y compared to G. The result suggests that the inhibition of enzyme activity of CHLP protein is
218 likely to further suppress the biosynthesis of Chl in G. In addition, Our physiological results show
219 that the content of Urogen III in the G is about 4 times than that of the Y, but the content of Coprogen
220 III is no significantly differed between G and Y. Therefore, there might be an interruption between
221 Urogen III and Coprogen III during Chl biosynthesis. However, the results need further verification.

222 Four enzymatic steps of the Chl catabolic pathway are that phytol, magnesium, and the
223 primary cleavage product of the porphyrin ring are catalyzed by Chlase, Mg-dechelatase,
224 pheophorbide a oxygenase, and red Chl catabolite reductase [41]. Chlase catalyzes the hydrolysis
225 ester bond of Chl to yield Chlide and phytol, is thought to be the first enzyme in the Chl degradation
226 [42]. Chlase activity is negatively correlated with Chl levels during citrus fruit color break and
227 Chlase participate in Chl breakdown of citrus [15]. However, some evidence does not support that
228 Chlase play a critical role in Chl degradation during leaf senescence [43-45]. For example,
229 overexpression of *ATHCOR1* which has Chlase activity in *Arabidopsis* led to an increased
230 breakdown of Chl a, but the total Chl level was not increased [43]. Similarly, *Arabidopsis* Chlases
231 (*AtCLH1* and *AtCLH2*) is not positively regulated with leaf senescence, *CHL1* and *CHL2* single and
232 double knockout mutant plants do not display a significant delay in senescence [44]. Schelbert et al.
233 also support the opinions that Chlase was not to be essential for dephytylation after Chl is converted
234 into pheophorbide [12]. In our study, the transcript expression patterns suggested that the
235 expression of *CLH* was higher in the Y than in the G. Moreover, previous studies in common wheat
236 (*Triticum aestivum* L.) showed that the gene encoding Chlase in the Chl biosynthesis pathway was
237 also significantly up-regulated in the yellow leaf mutant [45]. Therefore, experiments related to
238 cloning and functional verification of *CLH* in *Populus deltoides* Marsh are need to further verify the
239 function of Chlase in Chl breakdown.

240 3.2. The Expression Level of Genes Involved in Flavonoid Biosynthesis Were Altered in Leaf Color Mutants

241 Flavonoids, carotenoids, and Chls are the main pigments responsible for flower and leaf color.
242 Previous studies have demonstrated that flavonoids are the main pigments, producing purple, blue,
243 yellow, and red colors in plants [46]. Flavonoids have been known as UV-protecting pigments and
244 antioxidants by scavenging molecular species of active oxygen [47,48]. In *Ficus microcarpa* L. f., the
245 golden leaf mutant is the result of continuous high-light irradiation, and the flavonoid level of
246 golden leaf was 5-fold higher than that of green leaf, the results suggest that the increase of
247 flavonoids in the golden leaf may protect the leaves from high-light stress [49]. In this study, there is
248 no significant differences in the content of flavonoid between Y and G. Therefore, we consider
249 yellow leaf phenotype is caused by genetic factors, not environmental factors. Shikimate/quinic
250 hydroxycinnamoyltransferase (E2.3.1.133, HCT) belongs to the large family of BAHD-like
251 acyltransferases [50]. It is a key enzyme that determines whether 4-coumaroyl CoA is the direct
252 precursor for flavonoid or H-lignin biosynthesis [51]. In *Arabidopsis*, silencing of the *HCT* gene
253 resulted in severely reduced growth and absent S lignin [52]. The down-regulation of *HCT* have a
254 dramatic effect on lignin content and composition in alfalfa and poplar [53,54]. Up to now, Most
255 studies focus on the effects of *HCT* on lignin synthesis [55,56], while only a few studies related to the
256 *HCT* in flower color or leaf color of plants. It is further proved that the blocked Chl synthesis
257 pathway in Y may be the consequence of yellowing of the leaves.

258 4. Materials and Methods

259 4.1. *Plant materials and growing conditions*

260 The green leaf populus cultivar (wild-type) and the yellow leaf populus cultivar (mutant) were
261 used in this study. The plants were three-years-old and grown in Hongxia Nursery, Mianzhu Town,
262 Sichuan Province, China. Leaf tissues were collected in May, sampling three leaves per plant for five
263 plants of each type. All of the leaves were frozen immediately in liquid nitrogen after collection and
264 stored at -80°C for subsequent experiments.

265 4.2. *Measurements of Photosynthetic Pigments, Chl Precursors and flavonoid contents*

266 Approximately 0.1 g leaves of the G and Y were selected for Chl and carotenoid measurements.
267 The pigment (Chl a, Chl b, and carotenoid) contents were measured using the method described by
268 Lichtenthaler [57]. Coprogen III was extracted and determined as described by Bogorad [58]. To
269 measure the contents of Proto IX, Mg-Proto IX, Pchlide and Chlide a, leaves were ground into
270 powders with liquid nitrogen and submerged in nine volumes of phosphate-buffered saline (pH 7.4)
271 in an ice bath, then centrifuged (30 min at 8000 rpm). The supernatant was determined using ELISA
272 kit (MEIMIAN, Jiangsu, China) with a Thermo Scientific Multiskan FC (Thermo Fisher Scientific,
273 MA, USA). Flavonoid contents were measured using a UV1901 PCS Double beam UV-VIS
274 Spectrophotometer (Shanghai Yoke Instrument Co., Ltd., Shanghai, China) according to the
275 instructions of Favonoid Plant kit (Suzhou Comin Biotechnology Co., Ltd., Jiangsu, China). Three
276 biological replicates were evaluated for each sample. The data were analyzed using version 17.0 of
277 SPSS software (SPSS Inc., Chicago, IL, USA) with t test, and means were compared at the
278 significance levels of 0.01 and 0.05. The relative values of photosynthetic pigments and Chl
279 precursors in the Y use the value of G as control and calculated as 1.

280 4.3. *RNA extraction, quantification and qualification*

281 Total RNA was isolated from the G and Y leaves using CTAB extraction method. RNA
282 concentration and quality were checked using the Agilent 2100 Bioanalyzer (Agilent Technologies,
283 Santa Clara, USA). RNA purity was measured with a Nano Drop 2000 (Thermo Scientific, USA).

284 4.4. *Library preparation for transcriptome sequencing*

285 Two RNA samples were treated with DNaseI to remove any remaining DNA, and then the
286 oligo (dT) magnetic beads were used to collect poly A mRNA fraction. After mixing with
287 fragmentation buffer, the resulting mRNA was broken into short RNA inserts of approximately 200
288 nt. The fragments were used to synthesize the first cDNA strand via random hexamer priming, and
289 the second-strand cDNA was then synthesized using DNA polymerase I and RNase H. The cDNA
290 fragments was purified using magnetic beads and subjected to end-repair before adding a terminal
291 A at the 3ends. Finally, sequencing adaptors were ligated to the short fragments, which were
292 purified and amplified via polymerase chain reaction (PCR). The two libraries were generated and
293 then sequenced on an Illumina HiSeqTM 4000 platform by Chengdu Life Baseline Technology Co.,
294 Ltd. (Chengdu, China).

295 4.5. *Quality control and reads mapping*

296 The raw reads were edited to remove adapter sequences, low-quality reads, and reads with >10%
297 of Q < 20 bases, and then mapped using HISAT v2.0.0 software ([http://ccb.jhu.edu/
298 software/hisat2/downloads/](http://ccb.jhu.edu/software/hisat2/downloads/)) to the *Populus trichocarpa* Torr. & Gray genome.

299 4.6. *Quantification of gene expression level and differential expression analysis*

300 For gene expression analysis, gene abundance was estimated by RSEM v1.2.30 (<http://deweylab.github.io/RSEM/>)
301 and then normalized with fragments per kilobase of exon per million
302 mapped reads (FPKM) values [59]. To identify genes that were differently expressed between G and
303 Y, the NOIseq v2.16.0 ([http://www.bioconductor.org/packages/
release/bioc/html/NOISeq.html](http://www.bioconductor.org/packages/release/bioc/html/NOISeq.html))

304 was used in this experiment. Genes with probability >0.8 and $|\log_2 \text{fold change}| \geq 1$ were considered
305 as DEGs between samples.

306 For functional annotation, GO enrichment analysis of DEGs was performed in the GO database
307 (<http://www.geneontology.org/>) to calculate gene numbers for every term. The hypergeometric test
308 was conducted to find significantly enriched GO terms in the input list of DEGs. KEGG enrichment
309 analysis was implemented using the database resource (<http://www.genome.jp/kegg/>). The
310 calculation method of KEGG analysis is the same as the GO analysis.

311 4.7. Real-time RT-PCR

312 For qPCR analysis, total RNA was extracted using RNAPrep Pure Plant Kit (Tiangen Biotech Co.
313 Ltd., Beijing, China), approximately 1 μg RNA was reverse transcribed via a TransScript®
314 All-in-One First-Strand cDNA Synthesis SuperMix for qPCR (Tiangen Biotech Co. Ltd., Beijing,
315 China) according to the manufacturer's instructions. Eight genes were selected for validation using
316 qRT-PCR. Primer sequences were designed using Primer Premier 5.0 software as shown in Table S3.
317 qPCR DNA amplification and analysis were performed using the *TransScript*® Top Green qPCR
318 SuperMix kit (Tiangen Biotech Co. Ltd., Beijing, China) in accordance with the manufacturer's
319 protocol with an CFX Connect™ Real-Time System (Bio-Rad, Hercules, CA, USA). The thermal
320 profile was as follows: pre-denaturation at 94 °C for 30 s; 94 °C for 5 s, 60 °C for 30 s, for 40 cycles.
321 The relative expression level of selected genes in G and Y was normalized to CDC2 and ACT
322 expression. Three biological replicates for each of the reactions were performed. The relative
323 expression levels of target genes were estimated using the $2^{-\Delta\Delta C_t}$ method [60].

324 4.8. Data availability

325 All the clean reads is available at the National Center for Biotechnology Information (NCBI)
326 Short Read Archive (SRA) Sequence Database (accession number SRA740964). Supplemental files
327 available at FigShare. Table S1 contains significantly enriched gene ontologies among
328 downregulated or upregulated genes in Y type compared to G type. Table S2 contains pathway
329 enrichment. Table S3 contains primers for qPCR analysis.

330 5. Conclusions

331 In this study, physiological characterization and transcriptome sequence analysis showed that
332 there were distinct differences in coloration between green leaves and yellow mutant leaves of
333 *Populus deltoides* Marsh. Transcriptional sequence analysis identified 5 DEGs that participated in
334 porphyrin and Chl metabolism and flavonoid biosynthesis pathways. Furthermore, RT-qPCR
335 verified that those DEGs were expressed differentially in mutant and wild type plants.
336 Down-regulation of *CHLP* and up-regulation of *CLH* might cause the difference of leaves. These
337 results provide an excellent platform for future studies seeking for the molecular mechanisms
338 underlying the yellowing phenotype in *Populus deltoides* Marsh and other closely related species.

339 **Author Contributions:** F.Z. and S.Z. participated in the conceive and design the experiments; F.Z. supervised
340 the experiments; S.Z. performed the most experimental work and image analyses; X.W, J.C. and Q.L. analyzed
341 the transcriptomic data; X.W., Y. Z. and T. L. prepared the figures and tables; S.Z. wrote the paper. All authors
342 read and approved the final manuscript.

343 **Funding:** This research was funded by the National Natural Science Fund of China (No. 31870645) and by the
344 12th Five Year Key Programs for forest breeding in Sichuan Province (No. 2016YZGG).

345 **Conflicts of Interest:** The authors declare no conflict of interest.

346 Abbreviations

Chl Chlorophyll

DEGs	Differentially expressed genes
CHLP	Geranylgeranyl diphosphate
RT-qPCR	Quantitative real-time PCR
CHLD	Magnesium chelatase subunit D
CHLI	Magnesium chelatase subunit I
PORB	Protochlorophyllide oxidoreductase B
PPH	Pheophytinase
Chlase	Chlorophyllase
Urogen III	Uroporphyrinogen III
Coprogen III	Coproporphyrinogen III
Proto IX	Protoporphyrin IX
Mg-Proto IX	Magnesium protoporphyrin IX
Pchlde	Protochlorophyllide
Chlide	Chlorophyllide
G	Green leaves
Y	Yellow leaves
Caro	Carotenoid
CHLG	Chlorophyll synthase
PCR	polymerase chain reaction
NCBI	National Center for Biotechnology Information
SRA	Short Read Archive
FPKM	Fragments per kilobase of exon per million mapped reads

347 **References**

- 348 1. Li, Z.; Wang, J.; Zhang, X.; Xu, L. Comparative transcriptome analysis of anthurium “albama” and its
349 anthocyanin-loss mutant. *Plos One* **2015**, *10*, e0119027.
- 350 2. Li, W.; Yang, S.; Lu, Z.; He, Z.; Ye, Y.; Zhao, B.; Wang, L.; Jin, B. Cytological, physiological, and
351 transcriptomic analyses of golden leaf coloration in *Ginkgo biloba* L. *Hortic. Res.* **2018**, *5*.
- 352 3. Tanaka, Y., Sasaki, N., Ohmiya, A. Biosynthesis of plant pigments: anthocyanins, betalains and
353 carotenoids. *Plant Journal* **2008**, *54*, 733-749.
- 354 4. Tanaka, Y.; Brugliera, F.; Kalc, G.; Senior, M.; Dyson, B.; Nakamura, N.; Katsumoto, Y.; Chandler, S. Flower
355 color modification by engineering of the flavonoid biosynthetic pathway: practical perspectives. *Biosci.*
356 *Biotechnol. Biochem.* **2010**, *74*, 1760-1769.

- 357 5. Nagata, N.; Tanaka, R.; Satoh, S.; Tanaka, A. Identification of a vinyl reductase gene for chlorophyll
358 synthesis in *Arabidopsis thaliana* and implications for the evolution of Prochlorococcus species. *Plant Cell*
359 **2005**, *17*, 233-240.
- 360 6. Li, W.; Tang, S.; Zhang, S.; Shan, J.; Tang, C.; Chen, Q.; Jia, G.; Han, Y.; Zhi, H.; Diao, X. Gene mapping and
361 functional analysis of the novel leaf color gene SiYGL1 in foxtail millet [*Setaria italica* (L.) P. Beauv]. *Physiol.*
362 *Plant* **2015**, *157*, 24-37.
- 363 7. Wu, Z.; Zhang, X.; He, B.; Diao, L.; Sheng, S.; Wang, J.; Guo, X.; Su, N.; Wang, L.; Jiang, L.; et al. A
364 chlorophyll-deficient rice mutant with impaired chlorophyllide esterification in chlorophyll biosynthesis.
365 *Plant Physiol.* **2007**, *145*, 29-40.
- 366 8. Zhu, X.; Shuang, G.; Zhongwei, W.; Qing, D.; Yadi, X.; Tianquan, Z.; Wenqiang, S.; Xianchun, S.; Yinghua,
367 L.; Guanghua, H. Map-based cloning and functional analysis of YGL8, which controls leaf colour in rice
368 (*Oryza sativa* L.). *BMC Plant Biol.* **2016**, *16*, 134.
- 369 9. Luo, T.; Luo, S.; Araujo, W.L.; Schlicke, H.; Rothbart, M.; Yu, J.; Fan, T.; Fernie, A.R.; Grimm, B.; Luo, M.
370 Virus-induced gene silencing of pea CHLI and CHLD affects tetrapyrrole biosynthesis, chloroplast
371 development and the primary metabolic network. *Plant Physiol. Biochem.* **2013**, *65*, 17-26.
- 372 10. Yang, Y.L.; Xu, J.; Rao, Y.C.; Zeng, Y.J.; Liu, H.J.; Zheng, T.T.; Zhang, G.-H.; Hu, J.; Guo, L.B.; Qian, Q.; et al.
373 Cloning and functional analysis of pale-green leaf (PGL₁₀) in rice (*Oryza sativa* L.). *Plant Growth Regul.* **2016**,
374 *78*, 69-77.
- 375 11. Hörtensteiner, S. Update on the biochemistry of chlorophyll breakdown. *Plant Mol. Biol.* **2013**, *82*, 505-17.
- 376 12. Schelbert, S; Aubry, S; Burla, B; Agne, B; Kessler, F; Krupinska K, Hörtensteiner, S. Pheophytin
377 pheophorbide hydrolase (pheophytinase) is involved in chlorophyll breakdown during leaf senescence in
378 *Arabidopsis*. *Plant Cell* **2009**, *21*, 767-85.
- 379 13. Kariola, T.; Brader, G.; Li, J.; Palva, E.T. Chlorophyllase 1, a damage control enzyme, affects the balance
380 between defense pathways in plants. *Plant Cell* **2005**, *17*, 282-294.
- 381 14. Jacob-Wilk, D.; Goldschmidt, D.H.E.E.; Riov, J.; Eyal, Y. Chlorophyll breakdown by chlorophyllase:
382 Isolation and functional expression of the Chlase1 gene from ethylene-treated Citrus fruit and its regulation
383 during development. *Plant J.* **1999**, *20*, 653-661.
- 384 15. Azoulay Shemer, T.; Harpaz-Saad, S.; Belausov, E.; Lovat, N.; Krokhin, O.; Spicer, V.; Standing, K.G.;
385 Goldschmidt, E.E.; Eyal, Y. Citrus chlorophyllase dynamics at ethylene-induced fruit color-break: A study
386 of chlorophyllase expression, posttranslational processing kinetics, and in situ intracellular localization.
387 *Plant Physiol.* **2008**, *148*, 108-118.
- 388 16. Jung, K.-H.; Hur, J.; Ryu, C.-H.; Choi, Y.; Chung, Y.-Y.; Miyao, A.; Hirochika, H.; An, G. Characterization of
389 a Rice Chlorophyll-Deficient Mutant Using the T-DNA Gene-Trap System. *Plant Cell Physiol.* **2003**, *44*,
390 463-472.
- 391 17. Wang, P.; Gao, J.; Wan, C.; Zhang, F.; Xu, Z.; Huang, X.; Sun, X.; Deng, X. Divinyl chlorophyll(ide) a can be
392 converted to monovinyl chlorophyll(ide) a by a divinyl reductase in rice. *Plant Physiol.* **2010**, *153*, 994-1003.
- 393 18. Liu, W.; Fu, Y.; Hu, G.; Si, H.; Zhu, L.; Wu, C.; Sun, Z. Identification and fine mapping of a thermo-sensitive
394 chlorophyll deficient mutant in rice (*oryza sativa* L.). *Planta* **2007**, *226*, 785- 795.
- 395 19. Sakuraba, Y.; Rahman, M.L.; Cho, S.H.; Kim, Y.S.; Koh, H.J.; Yoo, S.C.; Paek N.C. The rice faded green leaf
396 locus encodes protochlorophyllide oxidoreductase and is essential for chlorophyll synthesis under high
397 light conditions. *Plant J.* **2013**, *74*, 122-133.
- 398 20. Sakuraba, Y.; Park, S.Y.; Kim, Y.S.; Wang, S.H.; Yoo, S.C.; Hrttensteiner, S.; Paek, N.C. *Arabidopsis*

- 399 stay-green2 is a negative regulator of chlorophyll degradation during leaf senescence. *Mol. Plant.* **2014**, 7,
400 1288-1302.
- 401 21. Zhang, K.; Liu, Z.; Shan, X.; Li, C.; Tang, X.; Chi, M.; Feng, H. Physiological properties and chlorophyll
402 biosynthesis in a pak-choi (*Brassica rapa* L. ssp. *chinensis*) yellow leaf mutant, *pylm. Acta Physiol. Plant.*
403 **2017**, 39, 22.
- 404 22. Akifumi, A.; Shozo, K.; Nami, G.Y.; Mikio, S.; Nobuhito, M.; Hiroshi, Y.; Yoshiko, K. Color recovery in
405 berries of grape (*vitis vinifera* L.) 'benitaka', a bud sport of 'italia', is caused by a novel allele at the
406 *VvmybA1* locus. *Plant Sci.* **2009**, 176, 470-478.
- 407 23. Wasscher, J. The importance of sports in some florist's flowers. *Euphytica* **1956**, 5, 163-170.
- 408 24. Li, C.F.; Xu, Y.X.; Ma, J.Q.; Jin, J.Q.; Huang, D.J.; Yao, M.Z.; Ma, C.L.; Chen, L. Biochemical and
409 transcriptomic analyses reveal different metabolite biosynthesis profiles among three color and
410 developmental stages in 'Anji Baicha' (*camellia sinensis*). *BMC Plant Bio.* **2016**, 16, 195.
- 411 25. Gao, M.; Hu, L.; Li, Y.; Weng, Y. The chlorophyll-deficient golden leaf mutation in cucumber is due to a
412 single nucleotide substitution in *CsChlI* for magnesium chelatase I subunit. *Theor. Appl. Genet.* **2016**, 129,
413 1-13.
- 414 26. Chen, H.; Cheng, Z.; Ma, X.; Wu, H.; Liu, Y.; Zhou, K.; Chen, Y.; Ma, W.; Bi, J.; Zhang, X.; et al. A knockdown
415 mutation of *YELLOW-GREEN LEAF2* blocks chlorophyll biosynthesis in rice. *Plant Cell Rep.* **2013**, 32,
416 1855-1867.
- 417 27. Zhang, S.; Zhi, H.; Li, W.; Shan, J.; Tang, C.; Jia, G.; Tang, S.; Diao, X. SiYGL2 is involved in the regulation of
418 leaf senescence and photosystem II efficiency in *Setaria italica* (L.) P. Beauv. *Front. Plant Sci.* **2018**, 9, 1308.
- 419 28. Zhang, L.; Liu, C.; An, X.; Wu, H.; Feng, Y.; Wang, H.; Sun, D. Identification and genetic mapping of a
420 novel incompletely dominant yellow leaf color gene, *Y1718*, on chromosome 2bs in wheat. *Euphytica* **2017**,
421 213, 141.
- 422 29. Ruan, B.; Gao, Z.; Zhao, J.; Zhang, B.; Zhang, A.; Hong, K.; Yang, S.; Jiang, H.; Liu, C.; Chen, G.; et al. The
423 rice *YCL* gene encoding an Mg²⁺-chelatase ChlD subunit is affected by temperature for chlorophyll
424 biosynthesis. *J. Plant Biol.* **2017**, 60, 314-321.
- 425 30. Yoshinobu, K.; Yasusi, Y.; Yasuko, S.; Ayumu, T.; Shunichi, T.; Hideo, Y. High-susceptibility of
426 photosynthesis to photoinhibition in the tropical plant *Ficus microcarpa* L. f. cv. golden leaves. *BMC Plant*
427 *Biol.* **2002**, 2, 2.
- 428 31. Wang, L.; Yue, C.; Cao, H.; Zhou, Y.; Zeng, J.; Yang, Y.; Wang, X. Biochemical and transcriptome analyses
429 of a novel chlorophyll-deficient chlorina tea plant cultivar. *BMC Plant Physiol.* **2014**, 14, 352.
- 430 32. Tanaka, A.; Tanaka, R. Chlorophyll metabolism. *Curr. Opin. Plant Biol.* **2006**, 9, 248-255.
- 431 33. Eckhardt, U.; Grimm, B.; Hortensteiner, S. Recent advances in chlorophyll biosynthesis and breakdown in
432 higher plants. *Plant Mol Biol.* **2004**, 56, 1-14.
- 433 34. Tanaka, A.; Ito, H.; Tanaka, R.; Tanaka, N.K.; Yoshida, K.; Okada, K. Chlorophyll a oxygenase (cao) is
434 involved in chlorophyll b formation from chlorophyll a. *Proc. Natl. Acad. Sci.* **1998**, 95, 12719-12723.
- 435 35. Masuda, T.; Fujita, Y. Regulation and evolution of chlorophyll metabolism. *Photochem Photobiol Sci.* **2008**, 7,
436 1131-1149.
- 437 36. von Wettstein, D.; Gough, S.; Kannangara, C.G. Chlorophyll biosynthesis. *Plant Cell* **1995**, 7, 1039-1057.
- 438 37. Addlesee, H.A.; Gibson, L.C.; Jensen, P.E.; Hunter, C.N. Cloning, sequencing and functional assignment of
439 the chlorophyll biosynthesis gene, *chl_p*, of *Synechocystis* sp. pcc 6803. *FEBS Lett.* **1996**, 389, 126-130.

- 440 38. Addlesee, H.A.; Hunter, C.N. Physical mapping and functional assignment of the
441 geranylgeranyl-bacteriochlorophyll reductase gene, *bchp*, of *rhodobacter sphaeroides*. *J. Bacteriol.*
442 **1999**, *181*, 7248.
- 443 39. Tanaka, R.; Oster, U.; Kruse, E.; Rudiger, W.; Grimm, B. Reduced activity of geranylgeranyl reductase leads
444 to loss of chlorophyll and tocopherol and to partially geranylgeranylated chlorophyll in transgenic tobacco
445 plants expressing antisense *rma* for geranylgeranyl reductase. *Plant Physiol.* **1999**, *120*, 695-704.
- 446 40. Shpilyov, A.V.; Zinchenko, V.V.; Shestakov, S.V.; Grimm, B.; Lokstein, H. Inactivation of the
447 geranylgeranyl reductase (*chlP*) gene in the cyanobacterium *Synechocystis* sp. pcc 6803. *BBA - Bioenergetics*
448 **2005**, *1706*, 195-203.
- 449 41. Harpazsaad, S.; Azoulay, T.; Arazi, T.; Benyaakov, E.; Mett, A.; Shibolet, Y.M.; Hortensteiner, S.; Gidoni,
450 D.; Galon, A.; Goldschmidt, E.E.; et al. Chlorophyllase is a rate-limiting enzyme in chlorophyll catabolism
451 and is posttranslationally regulated. *Plant Cell* **2007**, *19*, 1007-1022.
- 452 42. Tsuchiya, T.; Ohta, H.; Okawa, K.; Iwamatsu, A.; Shimada, H.; Masuda, T.; Takamiya, K. Cloning of
453 chlorophyllase, the key enzyme in chlorophyll degradation: finding of a lipase motif and the induction by
454 methyl jasmonate. *Proc. Natl. Acad. Sci. USA* **1999**, *96*, 15362-15367.
- 455 43. Benedetti, C.E.; Arruda, P. Altering the expression of the chlorophyllase gene *ATHCOR1* in transgenic
456 *Arabidopsis* caused changes in the chlorophyll-to-chlorophyllide ratio. *Plant Physiol.* **2002**, *128*, 1255-1263.
- 457 44. Schenk, N.; Schelbert, S.; Kanwischer, M.; Goldschmidt, E.E.; Dormann, P.; Hortensteiner, S. The
458 chlorophyllases *ATCLH1* and *ATCLH2* are not essential for senescence-related chlorophyll breakdown in
459 *Arabidopsis thaliana*. *FEBS Lett.* **2007**, *581*, 5517-5525.
- 460 45. Wu, H.; Shi, N.; An, X.; Liu, C.; Fu, H.; Cao, L.; Feng, Y.; Sun, D.; Zhang, L. Candidate genes for yellow leaf
461 color in common wheat (*Triticum aestivum* L.) and major related metabolic pathways according to
462 transcriptome profiling. *Int. J. Mol. Sci.* **2018**, *19*, 1594.
- 463 46. Sobel, J.M.; Streisfeld, M.A. Flower color as a model system for studies of plant evo-devo. *Front. Plant Sci.*
464 **2013**, *4*, 321.
- 465 47. Schmelzer, E.; Jahnen, W.; Hahlbrock, K. In situ localization of light-induced chalcone synthase mRNA,
466 chalcone synthase, and flavonoid end products in epidermal cells of parsley leaves. *Proc. Natl. Acad. Sci.*
467 *USA*. **1988**, *85*, 2989-2993.
- 468 48. Hernández, I.; Alegre, Leonor; Breusegem, V.; Frank. How relevant are flavonoids as antioxidants in
469 plants? *Trends Plant Sci.* **2009**, *14*, 125-132.
- 470 49. Yamasaki, H.; Heshiki, R. N. Leaf-goldenring induced by high light in *Ficus microcarpa* L.f., a tropical fig. *J.*
471 *Plant Res.* **1995**, *108*, 171-180.
- 472 50. D'Auria, J.C. Acyltransferases in plants: a good time to be BAHD. *Curr. Opin. Plant Biol.* **2006**, *9*, 331-340.
- 473 51. Li, X.; Bonawitz, N.D.; Weng, J.K.; Chapple, C. The growth reduction associated with repressed lignin
474 biosynthesis in *Arabidopsis thaliana* is independent of flavonoids. *Plant Cell* **2010**, *22*, 1620-1632.
- 475 52. Hoffmann, L.; Besseau, S.; Geoffroy, P.; Ritzenthaler, C.; Meyer, D.; Lapierre, C.; Pollet B.; Legrand, M.
476 Silencing of hydroxycinnamoyl-coenzyme A shikimate/quinate hydroxycinnamoyltransferase affects
477 phenylpropanoid biosynthesis. *Plant Cell* **2004**, *16*, 1446-1465.
- 478 53. Pu, Y.; Chen, F.; Ziebell, A.; Davison, B.H.; Ragauskas, A.J. NMR characterization of C3H and HCT
479 down-regulated alfalfa lignin. *BioEnergy Res.* **2009**, *2*, 198.

- 480 54. Peng, X.; Sun, S.; Wen, J.; Yin, W.; Sun, R. Structural characterization of lignins from hydroxycinnamoyl
481 transferase (HCT) down-regulated transgenic poplars. *Fuel* **2014**, *134*, 485-492.
- 482 55. Cui, K.; Wang, H.; Liao, S.; Tang, Q.; Li, L.; Cui, Y.; He Y. Transcriptome sequencing and analysis for culm
483 elongation of the world's largest bamboo (*dendrocalamus sinicus*). *Plos One* **2016**, *11*, e0157362.
- 484 56. Wu, Y.F.; Zhao, Y.; Liu, X.Y.; Gao, S.; Cheng, A.X.; Lou, H.X. Isolation and functional characterization of
485 hydroxycinnamoyltransferases from the liverworts *plagiochasma appendiculatum*, and *marchantia*
486 *paleacea*. *Plant Physiol. Biochem.* **2018**, *129*, 400-410.
- 487 57. Lichtenthaler, H.K. Chlorophylls and carotenoids: Pigments of photosynthetic biomembranes. *Methods*
488 *Enzymol.* **1987**, *148*, 350-382.
- 489 58. Bogorad, L. Porphyrin synthesis. In *Methods in Enzymology*; Colowick, S.P., Kaplan, N.O., Eds.; Academic
490 Press: New York, NY, USA, 1962; Volume 5, pp. 885-895, ISBN 0076-6879.
- 491 59. Mortazavi, A.; Williams, B.A.; McCue, K.; Schaeffer, L.; Wold, B. Mapping and quantifying mammalian
492 transcriptomes by RNA-Seq. *Nat Methods* **2008**, *5*, 621-628.
- 493 60. Schmittgen, T.D.; Livak, K.J. Analyzing real-time PCR data by the comparative C^T method. *Nat. Protoc.*
494 **2008**, *3*, 1101-1108.
- 495